

On single-mode Λ - and V-type micromasers: quantum interference versus photon statistics

Si-de Du^{1,2,3} and Yoshitaka Tanimura¹

¹ Theoretical Studies, Institute for Molecular Science, Myodaiji, Okazaki, Aichi 444-8585, Japan

² Department of Physics, Fudan University, Shanghai 200433, People's Republic of China

E-mail: sddu@fudan.ac.cn and sddu2002@hotmail.com

Received 3 April 2002, in final form 2 September 2002

Published 21 October 2002

Online at stacks.iop.org/JOptB/4/402

Abstract

Quantum interference effects are theoretically investigated in the steady-state photon statistics of single-mode Λ - and V-type micromasers with injected three-level atoms in a superposition of their internal states. The two lower (upper) levels are nondegenerate and coherent in a general case. For the Λ -type case, we have discussed how detunings affect the photon statistics of the *noninversion* micromaser. Under the proper conditions strongly sub-Poissonian field states with a large number of photons can be easily produced in this novel micromaser even if there exists no coherence between the two lower levels. For the V-type case, we have analysed how the photon statistics changes with the increase of the ground-state population. Although the generation of the strongly sub-Poissonian states is always possible in the micromaser under the noninversion case, their photon intensities become very weak compared to the Λ -type case. Our results indicate that it is perfectly possible to experimentally realize a noninversion micromaser with strongly sub-Poissonian statistics in the Λ -type system.

Keywords: Three-level atoms, micromasers, quantum interference, photon statistics

1. Introduction

The cavity quantum electrodynamics (QED) in the strong coupling regimes has become an important ground for testing fundamental thoughts of quantum physics. For recent advances in this field, for example, see the two papers in [1] and references therein. As is well known, the Jaynes–Cummings model (JCM) is the first fully quantum mechanical theoretical model which describes the interaction of a two-level atom with a single mode of the quantized electromagnetic field [2]. The JCM has been experimentally realized both in the microwave regime [3] and the optical regime [4]. This model is exactly solvable without any dissipation and under the rotating-wave approximation (RWA). Despite its simplicity, the JCM contains

many important phenomena, such as collapses and revivals [5], squeezing [6], sub-Poissonian statistics (SPS) [7], pure number states [8] and Schrödinger-cat states [9]. So far, the above phenomena, excluding squeezing, have been experimentally observed or produced in the one-atom maser during the past two decades [10–13].

The concepts of atomic coherence and interference have led to some surprising innovations in quantum optics [14], producing quantum noise quenching [15], lasers that emit squeezed light [16], lasing without population inversion [17] and new optical materials with a substantially enhanced index of refraction [18]. Recently, Fam Le Kien and his co-workers [19] have developed the quantum theory of the one-mode Λ -type micromaser for the case of two *degenerate* lower levels. They have predicted the field states with sub-Poissonian photon statistics in the micromaser without the need for a

³ Author to whom any correspondence should be addressed. Permanent address: Fudan University.

population inversion. This interesting phenomenon should be attributed to the atomic coherence between the two degenerate lower levels. Many experimental observations of amplification without inversion have been reported, for example, see [20]. So far as we know, however, a similar phenomenon has not yet been observed in micromasers experimentally.

The purpose of this paper is to investigate how quantum interference affects the steady-state photon statistics of single-mode Λ - and V-type micromasers with injected three-level atoms in a superposition of their states. In our models the two lower (upper) levels are *nondegenerate* and coherent in a general case. We show that the quantum interference can enhance the amplification of the photon intensity and sub-Poissonian (nonclassical) field states in the micromasers. A comparison is made between the Λ - and V-type micromasers. For the Λ -type case, the generation of sub-Poissonian field states with a large number of photons is always possible in the micromaser without the need for a population inversion *even if there exists no coherence between the two lower levels*. However, it is in general difficult for this phenomenon to take place in the V-type system *even if there exists strong coherence between the two upper levels*.

The rest of this paper is organized as follows. In section 2 we derive the master equations and present the steady-state photon-number distributions (PNDs). In section 3, based on the steady-state PNDs, we numerically investigate the photon intensity and its fluctuations. Our main results are summarized in section 4.

2. Master equations and steady-state PNDs

A true micromaser consists of a single-mode high- Q resonator in which a monoenergetic beam of excited atoms is injected at such a low flux that, at most, one atom at a time is present inside the cavity. In this paper the injected atom has Λ - and V-type three-level configurations, which are respectively presented in figures 1(a) and (b). E_1 , E_2 and E_3 are the energies of levels $|1\rangle$, $|2\rangle$ and $|3\rangle$, respectively; ω_0 is the frequency of the cavity field. For convenience, we use units of $\hbar \equiv 1$ throughout the paper. We assume that $\Delta = E_3 - E_2 \ll |E_3 - E_1|$ or $|E_2 - E_1|$. According to [21], one can obtain the effective Hamiltonian which describes the interaction of the cavity mode with an injected atom in the Λ - or V-type configuration under the RWA. For Λ type, the effective Hamiltonian is in the form

$$\hat{H}_{eff} = \Delta_1|3\rangle\langle 3| - \Delta_2|2\rangle\langle 2| + g_{12}(\hat{a}|1\rangle\langle 2| + \hat{a}^\dagger|2\rangle\langle 1|) + g_{13}(\hat{a}|1\rangle\langle 3| + \hat{a}^\dagger|3\rangle\langle 1|), \quad (1)$$

$$\Delta_1 = \omega_0 - (E_1 - E_3), \quad \Delta_2 = (E_1 - E_2) - \omega_0,$$

while it becomes for V type

$$\hat{H}_{eff} = \Delta_1|3\rangle\langle 3| - \Delta_2|2\rangle\langle 2| + g_{12}(\hat{a}|2\rangle\langle 1| + \hat{a}^\dagger|1\rangle\langle 2|) + g_{13}(\hat{a}|3\rangle\langle 1| + \hat{a}^\dagger|1\rangle\langle 3|), \quad (2)$$

$$\Delta_1 = (E_3 - E_1) - \omega_0, \quad \Delta_2 = \omega_0 - (E_2 - E_1).$$

In the above equations, \hat{a} and \hat{a}^\dagger are the photon annihilation and creation operators for the cavity field, g_{12} and g_{13} are the coupling strengths between the atom and field for two transition

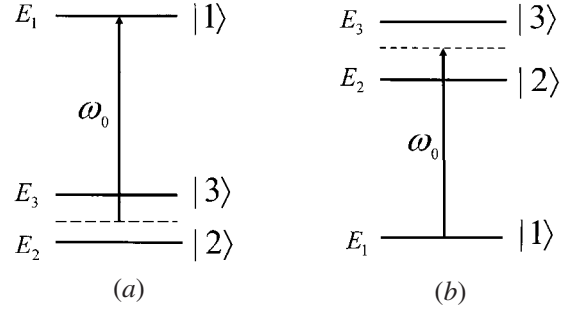


Figure 1. Atomic level configurations used throughout this paper: (a) Λ type and (b) V type.

processes and Δ_1 and Δ_2 are the detuning parameters between the field's frequency and the two atomic transition frequencies, respectively. In addition, $\Delta = \Delta_1 + \Delta_2$ is the energy difference between the two lower (upper) states.

We assume that, before entering the cavity, each atom is prepared in a mixed state. The density matrix of the initial state of each atom is given in the following form:

$$\rho_A = \rho_{11}^A|1\rangle\langle 1| + \sum_{i,j=2}^3 \rho_{ij}^A|i\rangle\langle j|, \quad (3)$$

where

$$\rho_{ii}^A > 0, \quad \sum_{i=1}^3 \rho_{ii}^A = 1, \quad (4)$$

$$\rho_{32}^A = \sqrt{\rho_{22}^A \rho_{33}^A} e^{i\phi} = \rho_{23}^{A*}.$$

In the above equation ϕ is a relative phase between levels 2 and 3. Let the atoms be injected into the cavity according to a Poissonian process with an average rate R . We denote the atom-field interaction time by τ . The coarse-grained equation of motion for the cavity field is then given by

$$\dot{\rho}(t) = R\delta_\tau\rho(t) + L\rho(t), \quad (5)$$

where $\delta_\tau\rho(t)$ is the change in $\rho(t)$ due to an atom interacting with the cavity field for the time τ , and $L\rho$ stands for the Liouvillian operator which describes losses due to the coupling of the cavity mode to a heatbath.

The change in $\rho(t)$ for the time τ is expressed by

$$\delta_\tau\rho(t) = \text{Tr}_{(A)}\{U(\tau)\rho_A \otimes \rho(t)U(\tau)^\dagger\} - \rho(t), \quad (6)$$

where $\text{Tr}_{(A)}$ is the trace with respect to atomic variables, and $U(\tau) = \exp(-i\hat{H}_{eff}\tau)$ is the evolution operator of the combined system.

The expression of the Liouvillian operator $L\rho$ is given by [14]

$$L\rho = \frac{1}{2}\Gamma(n_b + 1)(2\hat{a}\rho\hat{a}^\dagger - \hat{a}^\dagger\hat{a}\rho - \rho\hat{a}^\dagger\hat{a}) + \frac{1}{2}\Gamma n_b(2\hat{a}^\dagger\rho\hat{a} - \hat{a}\hat{a}^\dagger\rho - \rho\hat{a}\hat{a}^\dagger), \quad (7)$$

where Γ is the damping rate of the cavity mode and n_b is the number of thermal photons in the resonator.

Using equations (1)–(7), one can obtain the master equations for the Λ - and V-type micromasers. After a tedious

calculation, we find the equations of motion for the density-matrix elements which are suitable for both Λ type and V type

$$\begin{aligned} \dot{\rho}_{k,l} = & R[Q_1(k, l; \tau) + Q_2(k-1, l-1; \tau) - 1]\rho_{k,l} \\ & + RQ_3(k-1, l-1; \tau)\rho_{k-1, l-1} \\ & + RQ_4(k, l; \tau)\rho_{k+1, l+1} + \frac{1}{2}\Gamma(n_b + 1) \\ & \times [2\sqrt{(k+1)(l+1)}\rho_{k+1, l+1} - (k+l)\rho_{k,l}] \\ & + \frac{1}{2}\Gamma n_b [2\sqrt{kl}\rho_{k-1, l-1} - (k+l+2)\rho_{k,l}], \end{aligned} \quad (8)$$

but the related coefficients $Q_i(k, l; \tau)$ are obviously different for these two cases, which are given in the appendix, respectively.

Under the detailed balance, we can obtain the steady-state PND $P_n = \rho_{n,n}$ from equation (8). For Λ type, we have the following PND ($n \geq 1$):

$$P_n = P_0 \prod_{l=1}^n \frac{n_b + N_{ex}[\rho_{11}^A - Q_1(l-1, l-1; \tau)]/l}{(n_b + 1) + N_{ex}Q_4(l-1, l-1; \tau)/l}. \quad (9)$$

Similarly, one can obtain the following expression for V type ($n \geq 1$):

$$P_n = P_0 \prod_{l=1}^n \frac{n_b + N_{ex}Q_3(l-1, l-1; \tau)/l}{(n_b + 1) + N_{ex}[\rho_{11}^A - Q_2(l-1, l-1; \tau)]/l}. \quad (10)$$

In equations (9) and (10), $N_{ex} = R/\Gamma$ is the average number of atoms that traverse the cavity during the lifetime of the field and the probability P_0 is determined by the normalization condition $\sum_{n=0}^{\infty} P_n = 1$. Note that equation (9) can be reduced to the result of [19] when $\Delta_1 = \Delta_2 = 0$.

By making use of the theoretical treatment in this section, one can investigate photon statistics in the Λ - and V-type systems. In the following section we will investigate the photon statistics for the cavity mode. Without loss of generality, we assume that $g_{12} = g_{13} = g$. Moreover, we are only interested in the positive detunings. Throughout the present paper, the detunings Δ_1 and Δ_2 , and the energy difference Δ , are in units of g , while the interaction time τ is in units of g^{-1} .

3. Photon intensity and sub-Poissonian properties

In this section, based on equations (9) and (10), we numerically investigate the photon statistics by calculating the related averages. We define the normalized mean photon number \bar{n} and the normalized standard deviation of the photon distribution σ

$$\begin{aligned} \bar{n} = \langle n \rangle / N_{ex}, \quad \langle n \rangle = \sum_{n=0}^{\infty} n P_n, \\ \text{and} \quad \langle n^2 \rangle = \sum_{n=0}^{\infty} n^2 P_n, \quad (11) \\ \sigma = [\langle n^2 \rangle - \langle n \rangle^2 - \langle n \rangle] / \langle n \rangle, \end{aligned}$$

as a function of the dimensionless parameter θ given by

$$\theta = g\tau\sqrt{N_{ex}}/\pi, \quad (12)$$

which, in fact, plays the role of a pump parameter for the micromaser. For $\sigma = 0$, the field is Poissonian; for $\sigma > 0$,

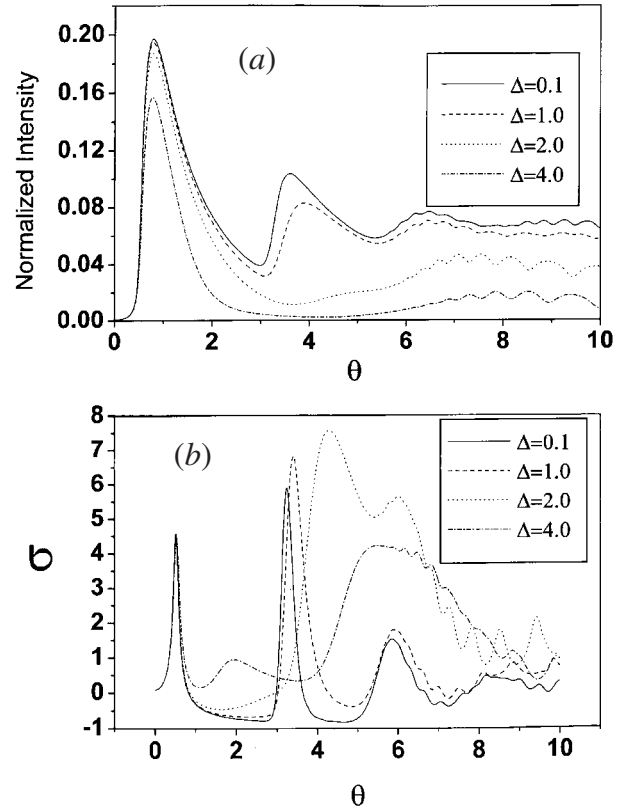


Figure 2. The normalized mean photon number \bar{n} (a) and the normalized standard deviation of the photon distribution σ (b) as a function of the dimensionless parameter θ for various symmetrical detunings when $\phi = \pi$, $\rho_{11}^A = 0.2$, $\rho_{22}^A = 0.4$, $N_{ex} = 200$ and $n_b = 0.1$.

the field is super-Poissonian; for $\sigma < 0$, however, the field is sub-Poissonian and nonclassical. On the other hand, the photon noises are enhanced for $\sigma > 0$, while they are reduced for $\sigma < 0$. In the following, we set $N_{ex} = 200$ and $n_b = 0.1$.

3.1. The Λ -type micromaser

In [19], the authors predicted sub-Poissonian field states in the *noninversion* Λ -type micromaser. Their theory is only suitable for the two *degenerate* lower levels. Now we discuss effects of the two *nondegenerate* lower levels on this interesting phenomenon and the photon intensity when $\phi = \pi$ and 0.

In figure 2, we show the change of \bar{n} and σ with the energy difference Δ ($\Delta_1 = \Delta_2$) when $\rho_{11}^A = 0.2$, $\rho_{22}^A = \rho_{33}^A = 0.4$ and $\phi = \pi$. As shown in figure 2, with increasing Δ , \bar{n} decreases, and the SPS becomes weak. When $\Delta = 4.0$, the SPS has disappeared although there is a significant amplification of the photon intensity in the region of small θ . Note that the strong SPS can exist in the cases of $\Delta \leq 2.0$. Therefore, the SPS is very sensitive to Δ when there is a very weak population in the excited state.

In order to understand the above results, we should note the physical meaning of Q_4 in equation (9). From equation (A.1), it is very obvious that Q_4 corresponds to the absorption from the lower levels $|2\rangle$ and $|3\rangle$ and to the interference between the channels of transitions. For $\rho_{22}^A = \rho_{33}^A$ and $\phi = \pi$, Q_4 is equal to zero due to the interference when $\Delta = 0$. In this case,

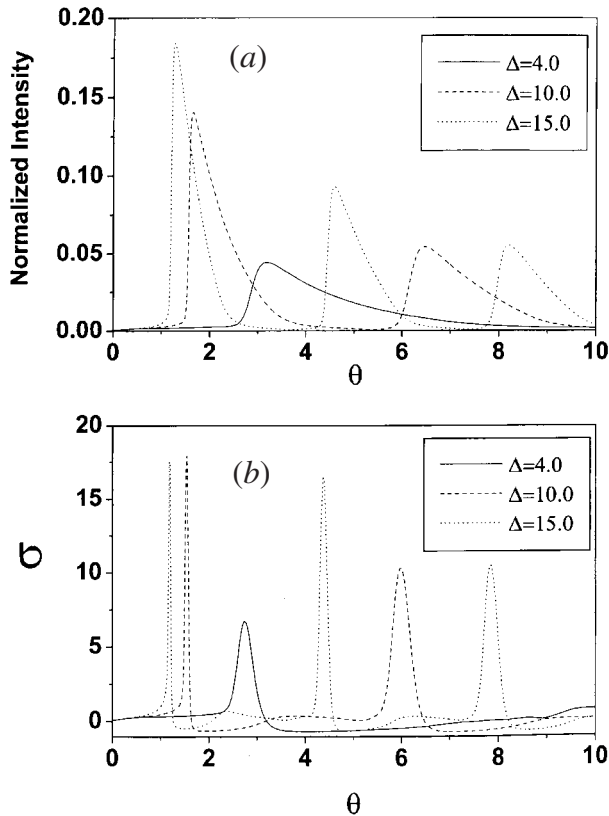


Figure 3. The normalized mean photon number \bar{n} (a) and the normalized standard deviation of the photon distribution σ (b) as a function of the dimensionless parameter θ for various symmetrical detunings when $\phi = 0$, $\rho_{11}^A = 0.2$, $\rho_{22}^A = 0.4$, $N_{ex} = 200$ and $n_b = 0.1$.

P_n is the largest and very different from the thermal photon distribution. With increasing Δ , Q_4 increases, so that P_n decreases. This is why \bar{n} decreases with increasing Δ . On the other hand, P_n tends to be like the thermal photon distribution with increasing Δ . Therefore, the SPS will disappear in larger Δ cases.

If Δ_1 is different from Δ_2 under the same Δ ($0.0 \leq \Delta \leq 4.0$), we found that there cannot exist a significant change in the photon statistics compared to the case of $\Delta_1 = \Delta_2$. This is very natural because there can only exist a slight difference between the two lower levels when Δ is very small.

For $\phi = 0$, this is another interference case. As Δ increases, in contrast, Q_4 becomes small and P_n is enhanced. Some interesting changes will occur in the photon statistics. This case is displayed in figure 3 ($\Delta \geq 4.0$). As Δ increases, the photon intensity is enhanced. For $\Delta = 15.0$, for example, the maximum \bar{n} is typically of the order of 0.2. From figure 3(b), we observe the very strong SPS. For $\Delta = 4.0$, the minimum σ is typically of the order of -0.7 although the maximum \bar{n} is only of the order of 0.05. With increasing Δ , the SPS appears more frequently, while a slight influence is imposed on the typical σ' value of -0.7 . We should point out that although $\Delta = 15.0$ is very large, our predictions are characteristic of the three-level system.

The trapping states (TSs) are another striking prediction on micromaser dynamics [22] and are experimentally observed [12]. This effect consists in a truncation of the PND at

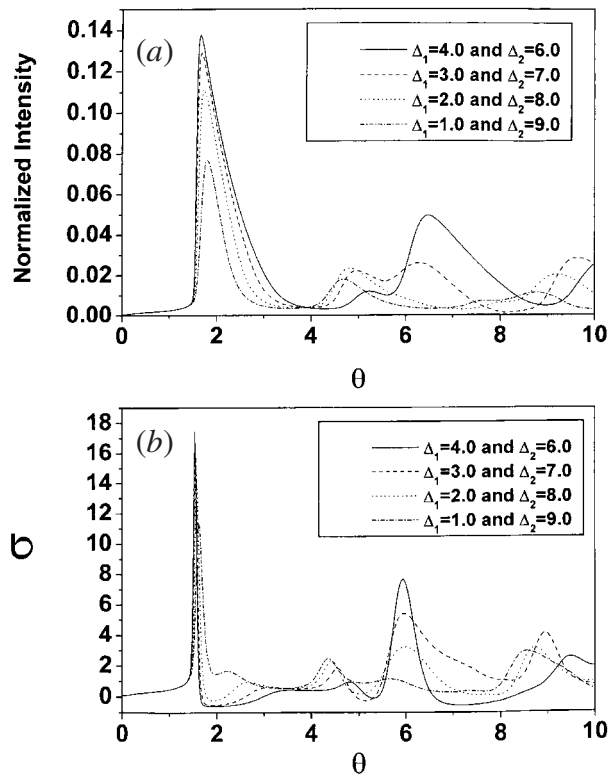


Figure 4. The normalized mean photon number \bar{n} (a) and the normalized standard deviation of the photon distribution σ (b) as a function of the dimensionless parameter θ for various asymmetrical detunings ($\Delta_1 + \Delta_2 = 10.0$) when $\phi = 0$, $\rho_{11}^A = 0.2$, $\rho_{22}^A = 0.4$, $N_{ex} = 200$ and $n_b = 0.1$.

particular values of the photon number. Typically, these states correspond to the sharp minima in the $\bar{n}-\theta$ space. However, we cannot observe such minima in figures 2(a) or 3(a). This is due to the detunings that make them broadened. As shown in figures 2(a) and 3(a), the large Δ cases have fully destroyed the TSs. We observe that the cavity mode is fundamentally at the thermal state of $n_b = 0.1$ in some intervals of the interaction time when $\Delta \geq 10.0$. This means that the injected atoms may be decoupled from the cavity mode at these times.

Based on figure 3, we now turn to the asymmetrical detunings ($\Delta_1 \neq \Delta_2$) when $\Delta = 10.0$ is fixed. This is presented in figure 4. For convenience, we define the deviation $\delta = |\Delta_1 - \Delta_2|$. As the deviation δ is enhanced, in general, both the photon intensity and the SPS become weaker and weaker. When $\Delta_1 = 1.0$ and $\Delta_2 = 9.0$, the maximum \bar{n} is typically of the order of 0.08, and the cavity mode has become super-Poissonian. However, we should mention that in the interval of θ from 4.0 to 6.0 the SPS becomes stronger in the case of $\Delta_1 = 3.0$ and $\Delta_2 = 7.0$ than in the case of $\Delta_1 = 4.0$ and $\Delta_2 = 6.0$. On the other hand, a significant influence is imposed on the TSs for large δ .

Even if there is no atomic coherence between the two lower levels, sub-Poissonian field states can be also produced in the *noninversion* Λ -type micromaser under the proper population of the excited state. This conclusion holds true for $0.5 \geq \rho_{11}^A \geq 0.45$ when the symmetrical detunings exist in the system. As shown later, the limit of ρ_{11}^A can be relaxed for some asymmetrical detunings. In figure 5 we present the change

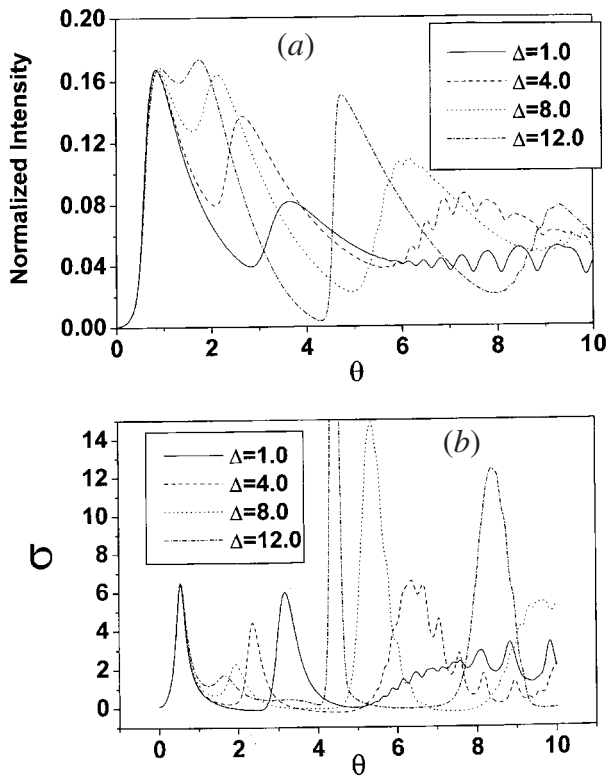


Figure 5. The normalized mean photon number \bar{n} (a) and the normalized standard deviation of the photon distribution σ (b) as a function of the dimensionless parameter θ for various symmetrical detunings when $\rho_{11}^A = 0.45$, $\rho_{22}^A = 0$, $N_{ex} = 200$ and $n_b = 0.1$.

in the photon statistics with Δ for the case of $\rho_{11}^A = 0.45$, $\rho_{22}^A = 0$ and $\rho_{33}^A = 0.55$. As seen from figure 5(a), a larger amplification of the photon intensity becomes possible in the micromaser with increasing Δ . For the SPS, the optimal degree is in turn equal to 11.0, 23.2, 22.8 and 10.0% for $\Delta = 1.0, 4.0, 8.0$ and 12.0; see figure 5(b). We note that it needs a longer interaction time for the larger Δ case to reach the optimal SPS.

Next we discuss the asymmetrical detunings when there is no atomic coherence between the two lower levels. We only deal with two cases: $\Delta_1 = 0$ (Δ_2 varies) and $\Delta_2 = 0$ (Δ_1 varies), which are presented in figures 6 and 7, respectively.

We observe from figure 6(a) that the curve is on the whole shifted up with the increase of Δ , which is very different from figure 5(a). It is obvious that the \bar{n} values in figure 6(a) are in general larger than the corresponding ones in figure 5(a) for the same Δ although they have the same population of the excited state. As shown in figure 6(b), the SPS becomes stronger and appears more frequently as Δ increases. This feature, of course, is very different from that in figure 5(b). The optimal SPS is in turn equal to 15.4, 30.6, 66.5 and 85.9% for $\Delta = 1.0, 4.0, 8.0$ and 12.0. This should be attributed to the fact that the system is undergoing a transition from the *three-level configuration without inversion* to the *effective two-level configuration with inversion* with increasing Δ . If $\Delta \gg g$, in fact, we can adiabatically eliminate the level $|2\rangle$. In this case the effective system is approximately equivalent to the two-level system with the excited state $|1\rangle$ of $\rho_{11}^A = 0.45$ and the ground state $|3\rangle$ of $\rho_{33}^A = 0$. Therefore the effective system has the net inversion of 45%. We note that under the proper Δ

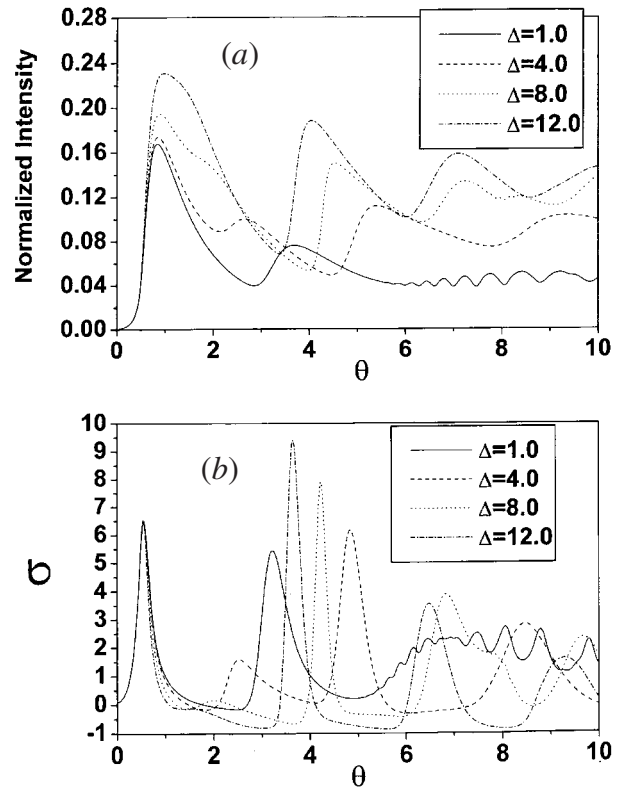


Figure 6. The normalized mean photon number \bar{n} (a) and the normalized standard deviation of the photon distribution σ (b) as a function of the dimensionless parameter θ when $\Delta_1 = 0$ and Δ_2 varies. Here $\rho_{11}^A = 0.45$, $\rho_{22}^A = 0.55$, $N_{ex} = 200$ and $n_b = 0.1$.

condition the present system is superior to the standard two-level system in the SPS even if the latter has the inversion of 100% [7]. It is found, on the other hand, that for the large Δ case the SPS can exist in the micromaser when the population of the excited state is reduced. For $\rho_{11}^A = 0.1$ and $\Delta = 12.0$, for example, the SPS can exist in a very wide interval of the interaction time from $\theta = 2.0$ to 7.4 and its degree is very high up to 70.9%. In this case \bar{n} is typically of the order of 0.05.

For $\Delta_2 = 0$ (Δ_1 varies), in contrast, the large Δ values are unfavourable to the photon statistics, specially to the SPS; see figure 7. When Δ is enhanced from 1.0 to 4.0, the optimal \bar{n} and SPS become stronger and stronger. As Δ is further enhanced from 8.0 to 12.0, however, they become weaker and weaker. For $\Delta = 12.0$, the SPS has disappeared, although the peak \bar{n} is large with the order of 0.1. These phenomena should be attributed to the fact that the system can be reduced to the *effective two-level configuration without population inversion* from the *three-level configuration without population inversion* with increasing Δ .

Finally, our investigation indicates that under the nondegenerate two lower levels it is always possible to produce the strong sub-Poissonian states with a large number of photons in the noninversion micromaser by adjusting θ , ϕ , Δ_1 and Δ_2 . We also note that in the two-level micromaser the SPS cannot exist in the noninversion case [23]. In the SPS, therefore, there exists a fundamental difference between the two-level micromaser and the three-level micromasers including the

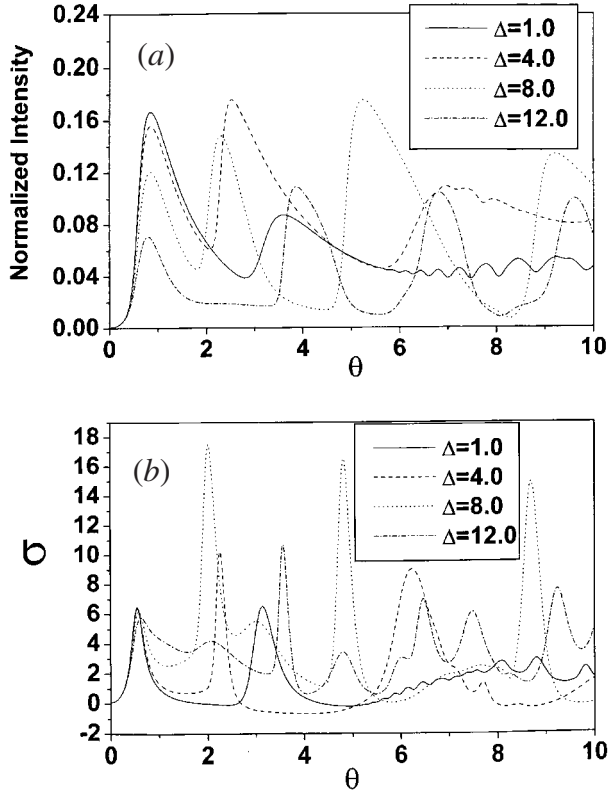


Figure 7. Same as figure 6 but when Δ_1 varies and $\Delta_2 = 0$.

V-type configuration which will be shown in the following subsection.

3.2. The V-type micromaser

We start discussing the V-type micromaser. We are only interested in the evolution of the photon statistics with the ground-state population. As shown above, $\rho_{22}^A = \rho_{33}^A$ and $\Delta_1 = \Delta_2$ are in general the optimal conditions for quantum interference. For atomic coherence, we are confined to the two extreme cases: the maximum constructive interference (MCI) ($\rho_{22}^A = \rho_{33}^A$ and $\phi = 0$) and the maximum destructive interference (MDI) ($\rho_{22}^A = \rho_{33}^A$ and $\phi = \pi$). We also treat the case without atomic coherence (CWAC) as a comparison.

For the full inversion ($\rho_{11}^A = 0.0$), we present the photon statistics for $\Delta_1 = \Delta_2 = 5.0$ in figure 8. On average, the MCI is the most favourable to the amplification of the cavity field, while the MDI is the most unfavourable; see figure 8(a). From figure 8(b), however, we observe that the MDI is the most favourable to the SPS because the latter can exist in longer time intervals and its degree is the strongest. We noted that the typical sub-Poissonian value is 89.8, 92.7 and 91.3%, respectively, for the MCI, MDI and CWAC. It is obvious that the SPS cannot exist in the MCI case for $\theta \geq 7.22$. It is interesting to note that there is one sharp minimum in the MCI although $\Delta_1 = \Delta_2 = 5.0$ is large. This means that the TS for the cavity mode may be existent in this interference case. However, one cannot see this phenomenon in the MDI and CWAC.

When a large population exists in the ground state, for example, $\rho_{11}^A = 0.3$, a significant influence is imposed on the

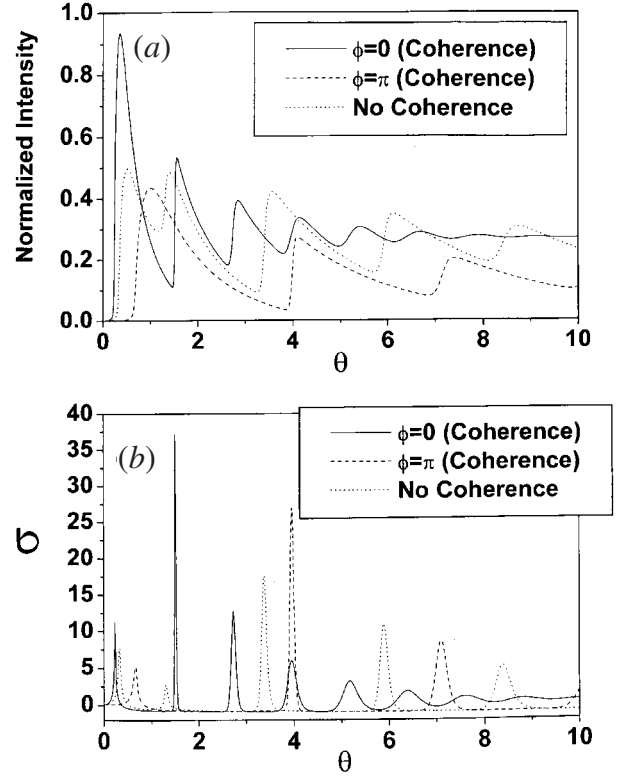


Figure 8. The normalized mean photon number \bar{n} (a) and the normalized standard deviation of the photon distribution σ (b) as a function of the dimensionless parameter θ when $\rho_{11}^A = 0$ and $\Delta_1 = \Delta_2 = 5.0$, $N_{ex} = 200$ and $n_b = 0.1$: $\phi = 0$, $\rho_{22}^A = \rho_{33}^A = 0.5$ for the solid curve; $\phi = \pi$, $\rho_{22}^A = \rho_{33}^A = 0.5$ for the dashed curve; $\rho_{22}^A = 0$, $\rho_{33}^A = 1.0$ for the dotted curve.

photon statistics; see figure 9. As shown in figure 9(a), the field intensity remarkably decreases in both the MCI and CWAC compared to the full inversion. In the CWAC the peak values are typically of the order of 5×10^{-2} . We note that the cavity field is fully around $n_b = 0.1$ in some intervals for the MCI and MDI. From figure 9(b), we observe that the SPS has become very weak in the MCI and disappeared in the CWAC. For the MCI, of course, the strong SPS is expected in the longer time behaviour. It should be noted that the cavity field is strongly sub-Poissonian up to 58% in the MDI.

We now turn to the noninversion cases. The case of $\rho_{11}^A = 0.52$ is presented in figure 10. From figure 10(a), we observe that the cavity field becomes very weak, specially for the MCI and CWAC. As seen from figure 10(b), the strong SPS can be found in the long-time behaviour for both the MCI and MDI. Obviously, the SPS can never exist in the CWAC.

We should discuss effects of the detuning parameters on the photon statistics in the micromaser. For the MCI, in general, the small symmetrical detunings are very helpful to both the light amplification and SPS. The detunings inversely become very detrimental to the SPS, however, if they are tiny. When $\rho_{11}^A = 0.52$ and $\rho_{22}^A = 0.24$, for example, the SPS can never exist in the double resonance ($\Delta_1 = \Delta_2 = 0$). For the MDI, in contrast, the large symmetrical detunings are favourable to the photon intensity and SPS. For the CWAC, if $\rho_{22}^A = 0$, the proper detuning deviations ($\Delta_1 = 0$) are very favourable to the light amplification and SPS. We investigated

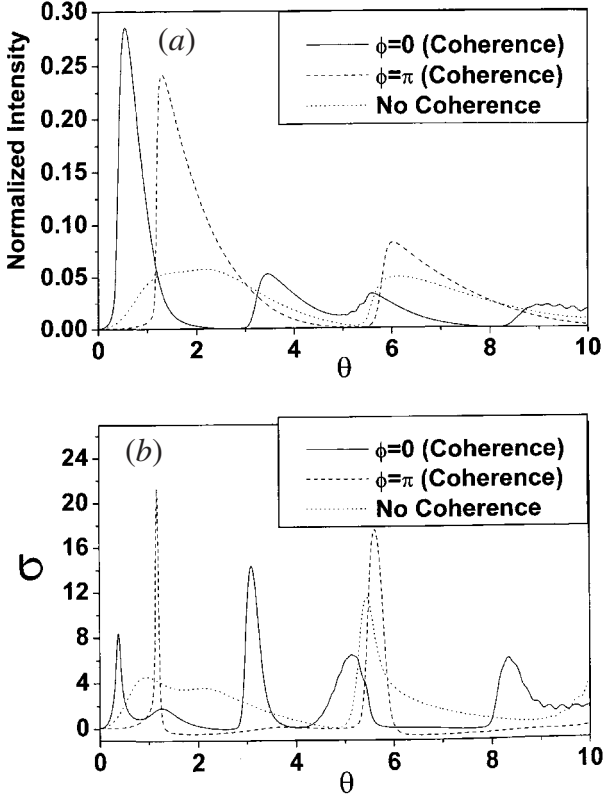


Figure 9. The normalized mean photon number \bar{n} (a) and the normalized standard deviation of the photon distribution σ (b) as a function of the dimensionless parameter θ when $\rho_{11}^A = 0.3$ and $\Delta_1 = \Delta_2 = 5.0$, $N_{ex} = 200$ and $n_b = 0.1$: (1) $\phi = 0$, $\rho_{22}^A = \rho_{33}^A = 0.35$ for the solid curve, (2) $\phi = \pi$, $\rho_{22}^A = \rho_{33}^A = 0.35$ for the dashed curve and (3) $\rho_{22}^A = 0$, $\rho_{33}^A = 0.7$ for the dotted curve.

the case when $\rho_{11}^A = 0.52$ and $\rho_{22}^A = 0$. As Δ is enhanced from 1.0 to 8.0 ($\Delta_1 = 0$), the largest \bar{n} approximately increases from 5×10^{-3} to 2×10^{-2} ($\theta \leq 30.0$). Although we observed field states with very strong SPS, the field intensity in these states is very weak.

In conclusion, the way in which the photon statistics responds to the change of the ground-state population is very different in the MCI, MDI and CWAC. On average, the light amplification and SPS in the quantum interference are superior to those in the CWAC. It is possible to realize the optical amplification in the noninversion micromaser even if there is no quantum interference between the atomic transitions. Although it is possible to produce the strongly sub-Poissonian field states in the noninversion micromaser, even in the CWAC, the field intensity in these states is so weak that it is difficult to observe them in an experiment.

4. Summary and discussion

In this paper we have investigated the photon statistics in the single-mode Λ - and V-type micromasers with injected three-level atoms in a superposition of their internal states. We have mainly discussed how the photon statistics responds to quantum interference between the two transition channels and compared the cases with and without quantum interference. Our main aspects are summarized as follows.

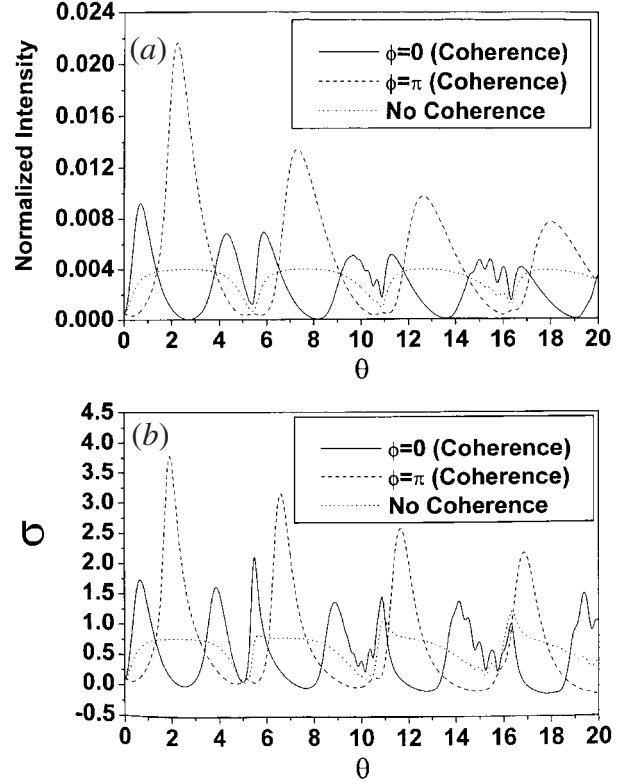


Figure 10. The normalized mean photon number \bar{n} (a) and the normalized standard deviation of the photon distribution σ (b) as a function of the dimensionless parameter θ when $\rho_{11}^A = 0.52$ and $\Delta_1 = \Delta_2 = 5.0$, $N_{ex} = 200$ and $n_b = 0.1$: (1) $\phi = 0$, $\rho_{22}^A = \rho_{33}^A = 0.24$ for the solid curve, (2) $\phi = \pi$, $\rho_{22}^A = \rho_{33}^A = 0.24$ for the dashed curve and (3) $\rho_{22}^A = 0$, $\rho_{33}^A = 0.48$ for the dotted curve.

- (1) We have derived the general analytical expressions for the PND in the Λ - and V-type cases, which are suitable for any detunings between the field frequency and atomic transition frequency.
- (2) For the Λ -type case, we have discussed how detunings affect the photon statistics of the noninversion micromaser. Under the proper conditions strongly sub-Poissonian field states with a large number of photons can be easily produced in this novel micromaser even if there exists no coherence between the two lower levels.
- (3) For the V-type case, we have analysed how the photon statistics changes with increasing ground-state population. Although the generation of the strongly sub-Poissonian states is always possible in the micromaser under the noninversion case, their photon intensities become very weak compared to the Λ -type case even if there is strong coherence between the two upper levels.
- (4) Compared to the case without atomic initial coherence, quantum interference can always enhance the photon intensity and SPS by choosing proper ϕ values under the same populations and detunings.
- (5) Our results indicate that it is perfectly possible to experimentally realize a noninversion micromaser with strongly sub-Poissonian statistics in the Λ -type system. However, it is perhaps very difficult to realize a similar micromaser in the V-type configuration. As is well

known, the field-intensity fluctuations (or shot noises) in the case with an inversion population are in general larger than those in the case without a inversion population. Therefore, the shot noises in this novel micromaser are significantly reduced, so that it will have a potential application to precise measurements.

Acknowledgments

The present investigations were supported by a Grant-in-Aid on Priority Area of Chemical Reaction Dynamics in Condensed Phases (10206210) and a Grant-in-Aid for Scientific Research (B)(12440171). SDD acknowledges that his work is in part supported by the National Natural Science Foundation of China under project nos 19804001 and 29833080. He also thanks Drs T Kato and Y Suzuki very much for their help.

Appendix

In this appendix, we will give the related coefficients $Q_i(k, l; \tau)$ in equation (8). For Λ type, we have

$$\begin{aligned}
 Q_1(k, l; \tau) &= \rho_{11}^A \sum_{\mu, v=1}^3 e^{-i\lambda_\mu(k)\tau + i\lambda_\nu(l)\tau} |A_\mu(k)|^2 |A_\nu(l)|^2, \\
 Q_2(k, l; \tau) &= \sum_{\mu, v=1}^3 e^{-i\lambda_\mu(k)\tau + i\lambda_\nu(l)\tau} E_{\mu, v}(k, l) \\
 &\quad \times [B_\mu(k)B_\nu(l)^* + C_\mu(k)C_\nu(l)^*], \\
 Q_3(k, l; \tau) &= \rho_{11}^A \sum_{\mu, v=1}^3 e^{-i\lambda_\mu(k)\tau + i\lambda_\nu(l)\tau} A_\mu(k)^* A_\nu(l) \\
 &\quad \times [B_\mu(k)B_\nu(l)^* + C_\mu(k)C_\nu(l)^*], \\
 Q_4(k, l; \tau) &= \sum_{\mu, v=1}^3 e^{-i\lambda_\mu(k)\tau + i\lambda_\nu(l)\tau} \\
 &\quad \times E_{\mu, v}(k, l) A_\mu(k) A_\nu(l)^*, \\
 E_{\mu, v}(m, n) &= \rho_{22}^A B_\mu(m)^* B_\nu(n) + \rho_{23}^A B_\mu(m)^* C_\nu(n) \\
 &\quad + \rho_{32}^A C_\mu(m)^* B_\nu(n) + \rho_{33}^A C_\mu(m)^* C_\nu(n), \\
 A_i(n) &= \frac{\lambda_i(n) + \Delta_2}{g_{12}\sqrt{n+1}} B_i(n) \equiv \tilde{A}_i(n) B_i(n), \\
 C_i(n) &= \frac{g_{13}[\lambda_i(n) + \Delta_2]}{g_{12}[\lambda_i(n) - \Delta_1]} B_i(n) \equiv \tilde{C}_i(n) B_i(n), \\
 B_i(n) &= 1/\sqrt{|\tilde{A}_i(n)|^2 + 1 + |\tilde{C}_i(n)|^2}.
 \end{aligned} \tag{A.1}$$

For V type, however, the corresponding coefficients are given by

$$\begin{aligned}
 Q_1(k, l; \tau) &= \sum_{\mu, v=1}^3 e^{-i\lambda_\mu(k)\tau + i\lambda_\nu(l)\tau} W_{\mu, v}(k, l) \\
 &\quad \times [\alpha_\mu(k)\alpha_\nu(l)^* + \beta_\mu(k)\beta_\nu(l)^*], \\
 Q_2(k, l; \tau) &= \rho_{11}^A \sum_{\mu, v=1}^3 e^{-i\lambda_\mu(k)\tau + i\lambda_\nu(l)\tau} |\gamma_\mu(k)|^2 |\gamma_\nu(l)|^2, \\
 Q_3(k, l; \tau) &= \sum_{\mu, v=1}^3 e^{-i\lambda_\mu(k)\tau + i\lambda_\nu(l)\tau} W_{\mu, v}(k, l) \gamma_\mu(k) \gamma_\nu(l)^*,
 \end{aligned}$$

$$\begin{aligned}
 Q_4(k, l; \tau) &= \rho_{11}^A \sum_{\mu, v=1}^3 e^{-i\lambda_\mu(k)\tau + i\lambda_\nu(l)\tau} \gamma_\mu(k) \gamma_\nu(l)^* \\
 &\quad \times [\alpha_\mu(k)\alpha_\nu(l)^* + \beta_\mu(k)\beta_\nu(l)^*],
 \end{aligned} \tag{A.2}$$

$$\begin{aligned}
 W_{\mu, v}(m, n) &= \rho_{22}^A \beta_\mu(m)^* \beta_\nu(n) + \rho_{23}^A \beta_\mu(m)^* \alpha_\nu(n) \\
 &\quad + \rho_{32}^A \alpha_\mu(m)^* \beta_\nu(n) + \rho_{33}^A \alpha_\mu(m)^* \alpha_\nu(n),
 \end{aligned}$$

$$\alpha_i(n) = \frac{g_{13}\sqrt{n+1}}{\lambda_i(n) - \Delta_1} \gamma_i(n) \equiv \tilde{\alpha}_i(n) \gamma_i(n),$$

$$\beta_i(n) = \frac{g_{12}\sqrt{n+1}}{\lambda_i(n) + \Delta_2} \gamma_i(n) \equiv \tilde{\beta}_i(n) \gamma_i(n),$$

$$\gamma_i(n) = 1/\sqrt{|\tilde{\alpha}_i(n)|^2 + |\tilde{\beta}_i(n)|^2 + 1}.$$

In equations (A.1), (A.2), $\lambda_i(n)$ is the i th root of the eigenvalue equation corresponding to equations (1) and (2). Note that equations (1) and (2) have the same eigenvalues due to symmetry. The expression of $\lambda_i(n)$ is easily found to be ($i = 1, 2$ and 3)

$$\begin{aligned}
 \lambda_i(n) &= 2\sqrt[3]{r} \cos \left[\eta + \frac{2}{3}(i-1)\pi \right] - \frac{\Delta_2 - \Delta_1}{3}, \\
 r &= \sqrt{-\left(\frac{\Omega}{3}\right)^3}, \quad \eta = \frac{1}{3} \arccos\left(-\frac{q}{2r}\right), \\
 \Omega &= -\left[\frac{1}{3}(\Delta_1^2 + \Delta_2^2 + \Delta_1\Delta_2) \right. \\
 &\quad \left. + g_{12}^2(n+1) + g_{13}^2(n+1)\right], \\
 q &= \frac{2}{27}(\Delta_2 - \Delta_1)^3 + \frac{\Delta_2 - \Delta_1}{3} \\
 &\quad \times [\Delta_1\Delta_2 + g_{12}^2(n+1) + g_{13}^2(n+1)] \\
 &\quad + [\Delta_1 g_{12}^2(n+1) - \Delta_2 g_{13}^2(n+1)].
 \end{aligned} \tag{A.3}$$

References

- [1] Hood C J, Lynn T W, Doherty A C, Parkins A S and Kimble H J 2000 *Science* **287** 1447
- [2] Pinkse P W H, Fischer T, Maunz P and Rempe G 2000 *Nature* **404** 365
- [3] Jaynes E T and Cummings F W 1963 *Proc. IEEE* **51** 89
- [4] First one-atom maser: Meschede D, Walther H and Müller G 1985 *Phys. Rev. Lett.* **54** 551
- [5] First one-atom laser: An K, Childs J J, Dasari R R and Feld M S 1994 *Phys. Rev. Lett.* **73** 3375
- [6] Eberly J H, Narozhny N B and Sanchez-Mondragon J J 1980 *Phys. Rev. Lett.* **44** 1323
- [7] Meystre P and Zubairy M S 1982 *Phys. Lett. A* **89** 390
- [8] Kuklinski J R and Madajczyk J L 1988 *Phys. Rev. A* **37** 3175
- [9] Rempe G and Walther H 1990 *Phys. Rev. A* **42** 1650
- [10] Filipowicz P, Javanainen J and Meystre P 1986 *Phys. Rev. A* **34** 3077
- [11] Krause J, Scully M O and Walther H 1987 *Phys. Rev. A* **36** 4547
- [12] Krause J, Scully M O, Walther T and Walther H 1989 *Phys. Rev. A* **39** 1915
- [13] Gea-Banacloche J 1990 *Phys. Rev. Lett.* **65** 3385
- [14] Gea-Banacloche J 1991 *Phys. Rev. A* **49** 5913
- [15] Raimond J M, Brune M and Haroche S 1997 *Phys. Rev. Lett.* **79** 1964
- [16] Observation of quantum collapse and revival in a one-atom maser: Rempe G, Walther H and Klein N 1987 *Phys. Rev. Lett.* **58** 353
- [17] Observation of sub-Poissonian photon statistics in a micromaser:

- Rempe G, SchmidtKaler F and Walther H 1990 *Phys. Rev. Lett.* **64** 2783
- [12] Preparing pure photon number states of the radiation field: Weidinger M, Varcoe B T H, Heerlein R and Walther H 1999 *Phys. Rev. Lett.* **82** 3795
- [13] Observing Schrödinger-cat states: Brune M, Hagley E, Dreyer J, Matre X, Maali A, Wunderlich C, Raimond J M and Haroche S 1996 *Phys. Rev. Lett.* **77** 4887
- [14] Scully M O and Zubairy M S 1997 *Quantum Optics* (Cambridge: Cambridge University Press)
- [15] Scully M O 1985 *Phys. Rev. Lett.* **55** 2802
Scully M O and Zubairy M S 1987 *Phys. Rev. A* **35** 752
- [16] Scully M O, Wódkiewicz K, Zubairy M S, Bergou J, Lu N and Meyer ter Vehn J 1988 *Phys. Rev. Lett.* **60** 1832
Bergou J, Benkert C, Davidovich L, Scully M O, Zhu S-Y and Zubairy M S 1990 *Phys. Rev. A* **42** 5544
- [17] Scully M O, Zhu S-Y and Gavrielides A 1989 *Phys. Rev. Lett.* **62** 2813
Bergou J A and Bogar P 1991 *Phys. Rev. A* **43** 4889
- [18] Scully M O 1991 *Phys. Rev. Lett.* **67** 1855
Fleischhauer M, Keitel C H, Scully M O, Su C, Ulrich B T and Zhu S-Y 1992 *Phys. Rev. A* **46** 1468
- [19] Fam Le Kien, Meyer G M, Scully M O and Walther H 1995 *Phys. Rev. A* **51** 1644
- [20] Zibrov A S, Lukin M D, Nikonov D E, Hollberg L, Scully M O, Velichansky V L and Robinson H G 1995 *Phys. Rev. Lett.* **75** 1499
- [21] Du Si-de, Zhou Lu-wei, Xu Zhi-zhan, Zhang Wen-qi and Li Yuan 1998 *J. Phys. B: At. Mol. Opt. Phys.* **31** 4895
- [22] Filipowicz P, Javanainen J and Meystre P 1986 *J. Opt. Soc. Am. B* **3** 906
- [23] Meystre P, Rempe G and Walther H 1988 *Opt. Lett.* **13** 1078
Fam Le Kien 1991 *Opt. Commun.* **82** 380